Development of a Fast Method for Optimization of Au Ball Bond Process

J. Gomes, M. Mayer, B. Lin

Department of Mechanical and Mechatronics Engineering, University of Waterloo, 200 University Ave. W. Waterloo, ON N2L3G1, Canada

Email: jjgomes@uwaterloo.ca

Abstract

An accelerated optimization method is developed to minimize required time and resources, and demonstrated for a 25 µm diameter Au ball bonding process. After a preparation phase to pre-set many parameters based on literature values, the values for more significant process parameters, impact force (IF) and EFO time (t_{EFO}) for a given target bond geometry are optimized in a second phase, utilizing a 3^2 full factorial experiment and the response surface method (RSM). The target bond strength of 120±2 MPa is achieved in a third phase by optimizing the ultrasonic energy (US) parameter using an iterative method. For an example process with a target geometry of 58 µm for the bonded ball diameter measured at the capillary imprint (BDC) and 16 µm for the height of the bonded ball (BH), the optimized process parameters (phases 2 & 3) can be found in less than 4 h. The values for IF and t_{EFO} are found to be 424 mN and 0.474 ms, respectively. The bond is strengthened with incrementing US until additional ball deformation occurs. The bond strength achieved is >120 MPa with 48.6% US. Other bonding parameters include EFO current (I_{EFO}) = 50 mA, temperature (T) = 158 °C, bond time (Bt) = 20 ms, and bond force (BF) = 185 mN.

1. Introduction

Wire bonding is the most widely used method for making interconnection in semi-conductor packaging with more than 80% of integrated circuits (ICs) using thermosonic wire bonding [1]. Gold (Au) has been the dominant bonding wire material since the beginning of wire bonding. However, the high price of Au has been pushing the wire bonding industry to look for alternative bonding wire materials. Copper (Cu) [2-6] silver (Ag) [7], and alloyed wires [8] have emerged as potential replacement to Au in recent years. With each new wire material, the bonding process is required to be re-qualified. In general, several process setup tasks are required before any mass production with new bonding wire can be started. The wire bondability is established by proper selection of equipment, materials, and process. Bond reliability is assured by accelerated aging tests. One of the demanding process setup tasks is ball bond optimization.

Six basic parameters of a typical ball bonding process can be used to determine basic profiles of electric flame-off (EFO) current, bond force, and ultrasonic energy, as shown in Fig. 1. These parameters include current amplitude and duration

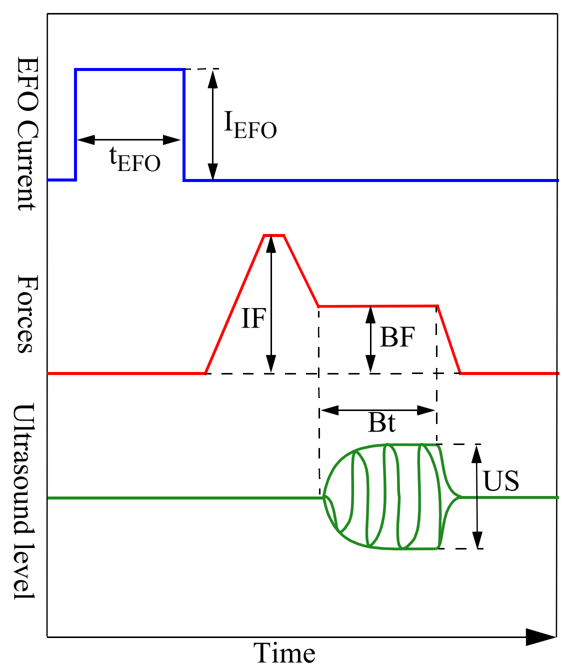

Fig. 1 Profiles of basic parameters for ball bond process

of the EFO spark (I_{EFO} and t_{EFO}, respectively) for free air ball (FAB) formation, impact force (IF) for FAB deformation, and bond force (BF), ultrasonic energy (US), and bond time (Bt) for bond formation. When the IF is substantially higher that the BF (double load profile), most of the ball deformation happens during impact in contrast to low IF process with deformation during ultrasonic bonding (US deformation) [9]. The process of bonding balls with mainly impact deformation is found to reduce cratering (a defect related to bonding stress) [9].

Optimization methods can include simple trial and error, full factorial design of experiment (DOE), response surface methodology (RSM), and numerical finite element analysis (FEA) [2-4, 10-15]. For example, a sequence of tests is carried out in [2] to optimize ball bond quality, starting with variable selection using an analysis of variance (ANOVA), followed by screening experiments, a fractional factorial DOE to find the detailed ranking of the process factors, and finally a central-composite type DOE combined with the response-surface-method to find process windows for the main factors. Such a stepwise approach has excellent results but requires substantial effort, and the adjustment of the geometry of the bonded balls was not described in [2].

More recent attempts to optimize the wire bonding process parameters are reported in [5] and [6]. In [5], an experimental design and grey relational analysis (GRA) is used to identify the relationship between process parameters and responses first, and then parameters are optimized using a fuzzy inference system and Taguchi method. The method provides superior optimization performance, however, it is a complex method requiring detail understanding of the process steps and the method did not focus on optimizing the bonded ball diameter. GRA is also used in [6] where an integrated neural network and genetic algorithm method is applied to achieve optimized parameters. Optimized parameters are then verified experimentally using RSM and excellent results are achieved. The method, however, is long and complex, and requires substantial amount of time and statistical understanding.

A method for a quicker verification of the bondability would be helpful when new types of wires are investigated. This study aims at applying existing process knowledge and models to develop a new method consisting of full factorial experiment, response surface method, and iteration resulting in faster ball bond optimization. This paper reports the details of a method that aims at making wire bonding studies more efficient, e.g. when process parameters need to be adjusted for different temperatures, wires, and substrates, or when machine-to-machine variations need to be identified. To completely setup a wire bonding process, many tasks are carried out with existing methods. The method presented here aims to be added to the existing methods for quicker and more accurate adjustment of ball bond geometry and strength.

2. Experimental

The bonding experiments are carried out on an ESEC 3100 automatic wire bonder (Besi, Cham, Switzerland). The capillary used is a commercial ceramic bottleneck capillary having a hole diameter of 35 μm and a chamfer diameter of 51 μm. The wire used is a 25 μm diameter 4N (99.99%) Au wire. Test chips used for the bonding process optimization are mounted on ceramic sidebrazed DIP substrates (Fig. 2). The aluminum (Al) metalized bonding pads contain 0.5% Cu dopant (Fig. 3). A total of 68 bond pads are used on each test chip. Bond sample size is typically five for the average and standard deviation values. The wedge bonds are made on the substrate terminals which are metalized with Au. All bonds are made at a nominal heater plate temperature of 175 °C. The actual temperature on bond pads is ≈158 °C.

The ball bond quality is measured based on bond geometry and shear strength (SS), and following JEDEC JESD22-B116A standard [16]. Dimensions measured include bonded ball diameter at capillary imprint (BDC) and bonded ball height (BH) as shown in Fig. 4. Values for shear force (SF) of ball bonds are measured in gramforce (gf) with a shear tester (1 gf = 9.81 mN). Bonds are shear tested in the direction perpendicular to the previously applied ultrasonic energy and towards the wedge bond [17]. Values for SS are calculated by dividing SF by an estimate of the cross-section area of the bond which is calculated from the BDC. Eq. 1 is used to normalize the shear test values so that the bond strengths can be compared from one ball size to another [1]. In this study, SS, SF, and BDC are measured in MPa, gf, and μm, respectively.

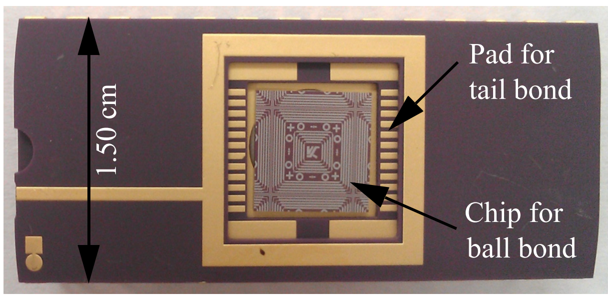

Fig. 2 Picture of test chip mounted on substrate

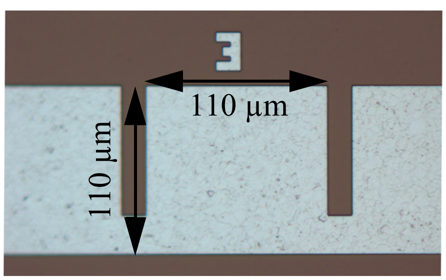

Fig. 3 Micrograph of ball bond pad (with dimensions) used for optimization

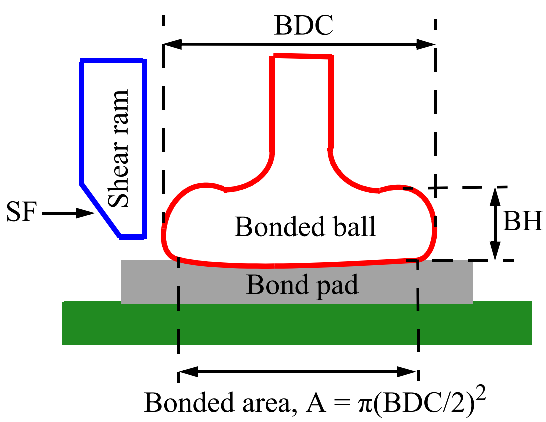

Fig. 4 Schematic defining dimensional parameters of ball bond

$$SS = \frac{SF}{\pi \times (BDC/2)^2} \qquad (1)$$

FAB diameters are measured in the x and y directions using optical micrograph as shown in Fig. 5, and the average of the Δx and Δy measurements is taken as the FAB diameter. Similar to the FAB measurement, the BDC is measured twice in orthogonal directions and the average is taken as shown in Fig. 6a. BH is measured from the change required to focus on the bottom and top of the ball bond (Figs. 6a & 6b).

Effective stress on the ball bond during bond formation can be quantified by dividing the BF value with the cross-sectional area of the bond which is measured by BDC. For the purpose of this study, Eq. 2 is developed to calculate that normal bond stress, σ_N, induced by the BF. In this study,

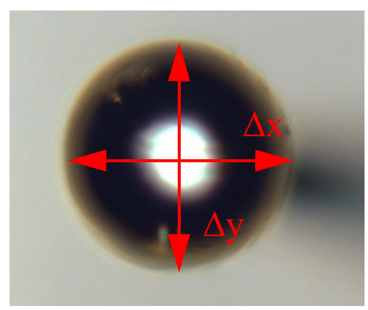

Fig. 5 Micrograph of typical FAB, used for diameter measurement

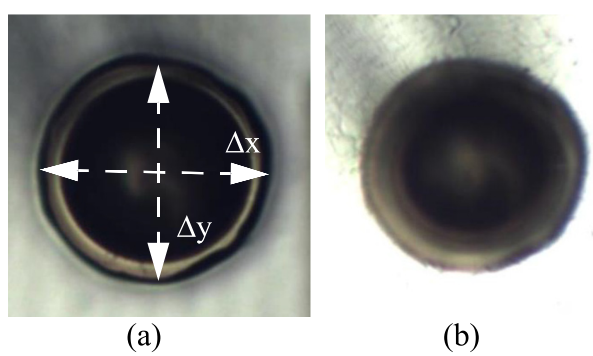

Fig. 6 Example micrographs of typical ball bond, (a) focus on top for diameter measurement, and (b) focus on the pad for height measurement

σ_N, BF, and BDC are measured in MPa, mN, and µm, respectively.

$$\sigma_N = \frac{BF}{\pi \times (BDC/2)^2} \qquad (2)$$

The value for the ultrasonic amplitude is given in "%", where 1% is equivalent to a peak-to-peak vibration amplitude of 26.6 nm measured at the center of the transducer tip [9].

An overview of the optimization method of ball bond along with target responses is given in Table 1. The detail methodology is described in following sections.

3. Preparations

The target bonded ball diameter is chosen 52 µm smaller than the bond pad opening, resulting in a value of 58 µm. Standard engineering practice for the height to diameter ratio for the bond suggests values between 1:4 and 1:3, which means bonded ball height (BH) should be between 19.3 µm to 14.5 µm [18, 19]. The target height chosen for this optimization method is 16 µm which lies in between those two values. The wedge bond process is setup by trial-and-error. Bond temperatures and looping parameters are adjusted in a similar way as in [18, 20]. Table 2 shows the preparation stage parameters.

Previous studies have found that a normal bond stress (σ_N) of about 70-75 MPa induced by BF is best for bond strength and reduction of underpad stress [19, 21]. The required BF inducing 70 MPa bond stresses on a ball with BDC = 58 µm is 184.9 mN as determined using Eq. (2). Based on this, the BF selected for the optimization method is 185 mN.

4. Obtaining Target Bond Geometry

A 3^2 full factorial experiment is used to obtain the target geometry [22]. The two factors of the factorial experiment are IF and t_{EFO} and the response of interests are the resultant BDC and BH. Alternatively, I_{EFO} could be used as a factor when t_{EFO} is kept constant. For this study, impact

Table 2 Bond parameters including values from preparation stage

	Parameters	Values
Wedge Bond	Impact Force (IF) [mN]	400
	Bond Force (BF) [mN]	300
	Bond Time (Bt) [ms]	20
	Ultrasonic Power (US) [%]	40
EFO	EFO Current (I_{EFO}) [mA]	50
	Elec.-wire Dist. (EWD) [µm]	100
	Tail Length (TL) [µm]	500
	EFO Time (t_{EFO}) [ms]	To be optimized
Ball Bond	Bond Force (BF) [mN]	185
	Bond Time (Bt) [ms]	20
	Pre-Ultrasonic [%]	0
	Impact Force (IF) [mN]	To be optimized
	Ultrasonic Power (US) [%]	To be optimized

Table 1 Suggested sequence of steps for fast optimization of ball bonds

Step	Description	Based on	Details in
1. Selecting target responses with tolerances and unoptimized process parameters	Larger pitch bonding process with BDC = 58±1 µm, BH = 16±1 µm, and SS = 120±2 MPa is chosen. Unoptimized bonding parameters are chosen from literature and experience.	Product requirements	Section 3
2. Optimizing parameters for target geometry	IF and t_{EFO} are optimized using a full factorial experiment at low US level. Values for factor levels are selected from process knowledge.	Bonding experiments	Section 4
3. Adjusting parameters for target bond strength	Bonds are strengthened by gradual increment of US till bond geometry surpasses acceptable range. US value resulting in SS equal to the target value is selected to be optimum.	Bonding experiments	Section 5

deformation bonding process is used and the IF values selected for the experiment are 278 mN, 370 mN, and 462 mN, which are approximately 1.5, 2, and 2.5 times the BF. The range of the IF factor was chosen based on the following considerations: no BDC was observed on the bonds for IF < 270 mN indicating a minimum level for IF, and bonds were severely deformed and breaking near the neck region when IF > 465 mN indicating a maximum IF level. The maximum t_{EFO} value for the experiment is 0.49 ms which produces FAB diameter ≈50 µm (2 x wire diameter) [1, 9, 18, 19] and is confirmed visually with bonder microscope as shown in Fig. 7. Remaining t_{EFO} values are 0.46 ms and 0.43 ms which are 0.03 ms and 0.06 ms smaller than the maximum value respectively. The range for t_{EFO} was determined by trial and error and to be large enough to obtain significant variation in responses. In particular, the FAB diameters obtained with 0.46 ms and 0.43 ms are ≈48 µm and ≈46 µm, respectively.

In order to minimize or even prevent ultrasonic enhanced deformation (UED), the factorial experiment is performed at a minimal US level. Test bonds for each set of parameters are made at constantly decreasing US until some of the ball bonds no longer stick to the bond pad (NSOP) which occurs at 25% US. At this point, the US is increased by 5% to 30% at which level no NSOPs are observed.

Five samples are prepared for each combination of IF and t_{EFO}, and BDC and BH are measured. The average BDC and BH values with one standard deviation are shown in Table 3.

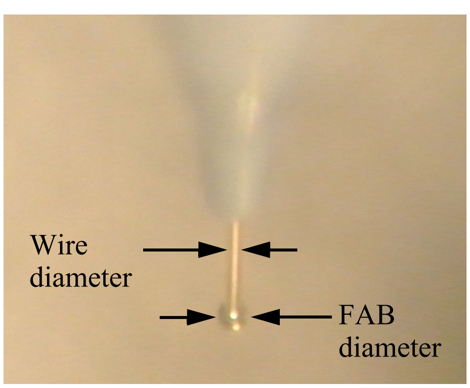

Fig. 7 Micrograph of FAB in the bonder prepared with t_{EFO} = 0.49 ms and I_{EFO} = 50 mA.

A contour plot is shown in Fig. 8 with the average values of BDC and BH plotted against IF and t_{EFO}. The overlapping lines are isolines for constant BDC and BH values. The intersection point of the isolines for target BDC (58 µm) and BH (16 µm) gives the optimized IF (IF^{Opt} = 424±5 mN) and (t_{EFO}^{Opt} = 0.474±0.013 ms) values that are now tested with minimal US (30%) for confirmation. The average results are within the specified target values (Table 4). The error values for IF^{Opt} and t_{EFO}^{Opt} are derived from the standard error associated with the average values of BDC and BH.

Table 3 BDC [µm] and BH [µm] (shown in italics) at different t_{EFO} and IF combination (± values are one standard deviation)

IF [mN]	t_{EFO} [ms] 0.43	0.46	0.49
278	53.54±1.10 *15.0±1.0*	54.71±0.68 *17.4±1.3*	56.97±0.80 *20.8±0.8*
370	54.45±0.51 *13.8±1.1*	56.54±0.24 *15.4±1.1*	57.79±0.87 *19.2±1.3*
462	57.20±0.91 *12.8±0.8*	58.17±0.56 *14.4±0.5*	59.59±0.91 *17.2±0.4*

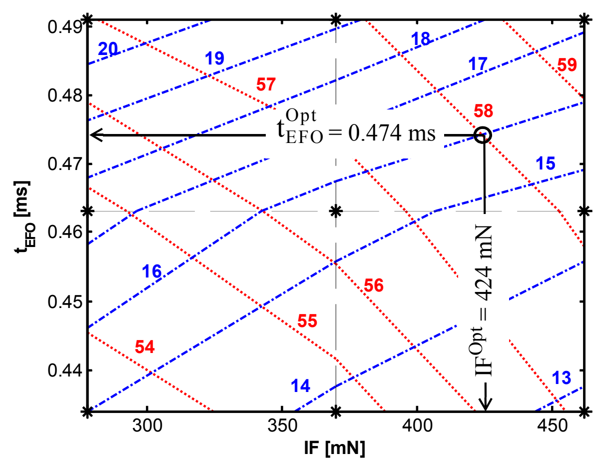

Fig. 8 Contour plot of BDC (red dotted lines) and BH (blue dashed lines). Intersection between target BDC (58 µm) and BH (16 µm) gives optimized IF and t_{EFO} parameters, at minimal US (30%), Star (*) points indicate treatment locations

5. Bond Strength Maximization

Bond strength is maximized by increasing the US from the minimal level (30%) to a level more than double (e.g. 80%) with a sufficiently small increment, e.g. 10%. The BDC and BH as a function of US shown in Fig. 9. The SF and SS values are plotted against the respective US levels in Fig. 10. The SS is expected to have its maximum near 50% US. Above 50% US, there is a sharp increase in BDC and decrease in BH is observed Fig. 9. The US corresponding to the target SS (120 MPa) is found to be 48.6% (Fig. 10).

The percent deviation between target values and resultant values from verification bonds made with 48.6% US are <3% as shown in Table 5. The average SS value is within the target range of 120±2 MPa.

6. Accelerated Optimization

The optimization method from the previous section is developed with measurements from a total of 110 bonded balls. Of the 110 bonded balls, 35 are sheared. The whole method takes about four hours to complete. To reduce this time, a number of simplification steps are described.

Sample size can be reduced by using a 2^2 factorial experiment instead of a 3^2. To show the adequacy of a 2^2 experiment, a 2^2 subset of data is taken from the 3^2 results. In this 2^2 experiment, IF is either 278 mN or 462 mN, the t_{EFO} is either 0.43 ms or 0.49 ms. The intersection point of target BDC and BH isolines gives the optimized IF (418 mN) and t_{EFO} (0.468 ms), which are less than 2% different from those obtained with the 3^2 experiment.

Confirmation bonds are made with these new parameters and the resultant FAB, BDC, and BH values are within the target responses, indicating that the 2^2 factorial experiment provides response values sufficiently close to those of the 3^2 experiment. Hence, it is possible to find acceptable opti-

Table 4 Measured geometries of confirmation bonds at optimized IF (424 mN) and t_{EFO} (0.474 ms) and minimal US (30%) (±values are one standard deviation)

FAB dia. [µm]	BDC [µm]	BH [µm]
49.67±0.37	57.29±0.47	15.6±0.89

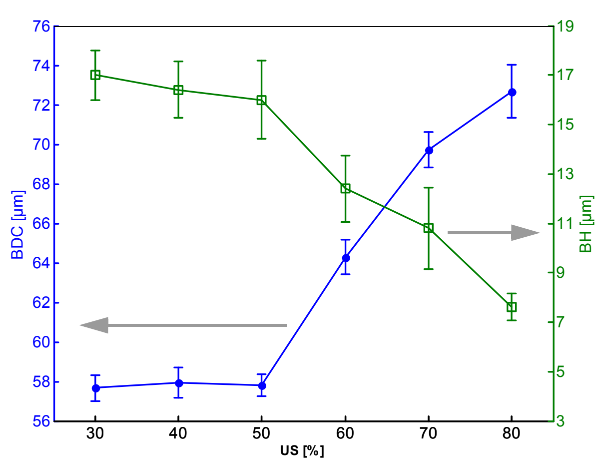

Fig. 9 Plot showing BDC and BH measured at different US level (5 measurements per level)

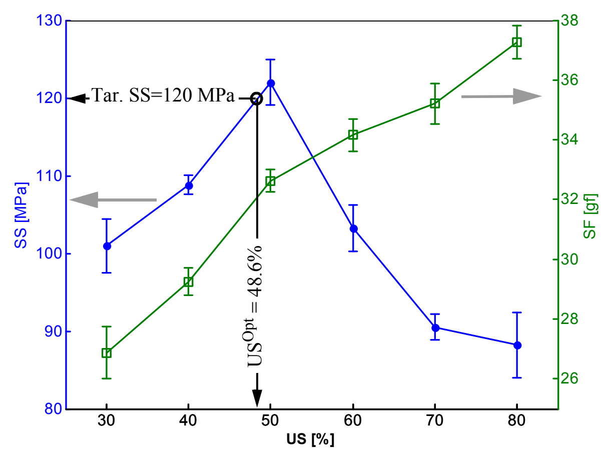

Fig. 10 Plot showing SF and SS measured at different US level (5 measurements per level). Optimized US of 48.6% deduced from target SS of 120 MPa

Table 5 Measured bond geometry and strengths at optimized US (48.6%). Comparison between the average measured values and the target values are shown as well

	Resultant	Target	Deviation [%]
BDC [µm]	58.06±0.37	58±1	~0.1
BH [µm]	15.6±1.1	16±1	~2.5
SS [MPa]	118.12±1.96	120±2	~1.6

mized parameters with 2^2 factorial experiments to reduce the second step of the optimization method to 20 bonded balls.

It is possible to further reduce the required measurements significantly via careful observation of bonded balls on the process microscope on the bonder. In the bond strength maximization step, UED can be detected optically and bonds at higher US levels can be avoided. In the context of this study, US optimization could be stopped after 60% US since the change on BDC shape is significant and visually detectable. So, bonds performed at 70% and 80% are redundant, since the optimum US level would not be larger than 60%. This means an optimum US can be found using only 20 bonds.

Applying the simplification steps reduces method duration to ≈152 minutes with acceptable optimized parameters. A detailed breakdown of the efforts for developed phase and suggested accelerated method is shown in Table 6.

7. Limitations of the Method

While effective in quickly determining optimized process parameters to obtain a pre-selected set of target responses, the method does not provide process windows which are often required to control wire bonding in mass production.

Also, all the measurements are performed within one day. Hence, day-to-day variation or chip-to-chip variation that can occur in same applications are not captured with the amount of measurements used in this study as it is not large enough. However, if the method is repeated, then it can be used to quantify the variations of the process.

The optimization method can be followed by a reliability assessment. Moreover, the method possibly needs to be adjusted for other wire materials (e.g., Cu, Ag, etc.) since it is developed with Au wire. In order to verify the applicability of the method on other types and sizes of wire materials, accelerated optimization is carried out on 20 μm 4N (99.99% Cu) palladium coated copper (PCC) wire on the same bond pad material. Shielding gas with flow rate of 0.5 l/min is used to prevent oxidation during FAB formation [9]. The results obtained are summarized in Table 7, suggesting that the presented optimization method can be applicable to Cu wire. A micrograph of a typical optimized PCC ball bond is shown in Fig. 11.

8. Conclusion

An accelerated method is developed to optimize key ball bond parameters (IF, t_{EFO}, and US) for target bond geometry and strength. It is evident that effective and non-exhaustive optimization method can be developed by utilizing existing knowledge of the wire bonding process. As the method is quick, it lends itself to study different aspects of wire bonding more thoroughly. The next

Table 6 Detail breakdown of experimentation time and test bonds required to complete optimization process

Experimental steps	Tasks performed	Development phase		Accelerated demonstration	
		Time [min]	No. of Bonds	Time [min]	No. of Bonds
Obtaining target bond geometry	Minimizing US until NSOP to prevent UED	28	25	28	25
	3^2 factorial experiment to optimize IF and t_{EFO}	62	45	28	20
	Analyzing measured BDC and BH	20		10	
	Confirmation FAB and bonds	17	5	17	5
Bond strength maximization	Increasing US and measure bond geometry	37	30	24	20
	Shear force measurement	19		13	
	Processing data to obtain optimum US	20		15	
	Confirmation bonds	17	5	17	5
Total		**220**	**110**	**152**	**75**

step is to apply the method for finer pitch process and different wire materials and make adjustments if necessary. For example, the effects of shielding gas flow rate need to be considered while optimizing parameters for fine pitch Cu wire bonding. Moreover, long term reliability of the optimized bonds needs to be addressed in future works.

Acknowledgments

This work is supported by the Natural Science and Engineering Research Council (NSERC) Canada, Microbonds Inc. (Markham, Canada), and Initiative for Automotive Manufacturing Innovation (IAMI), Ontario, Canada. The support with samples from Kulicke & Soffa Industries Inc. (PA, USA) is gratefully acknowledged.

Table 7 **Results of fast optimization method for PCC wire (± values are one standard deviation)**

	Definitions	Values
Target	BDC [μm]	45±1
	BH [μm]	12±1
	SS [MPa]	> 120
Bond parameters	BF [mN]	112
	Bt [ms]	10
	I_{EFO} [mA]	50
	IF^{Opt} [mN]	347±9
	t_{EFO}^{Opt} [ms]	0.395±0.003
	US^{Opt} [%]	45
Resulted	BDC [μm]	44.41±0.94
	BH [μm]	11.6±0.7
	SS [MPa]	133.8±6.5

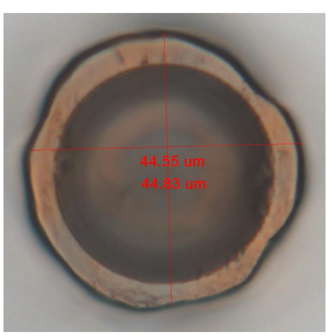

Fig. 11 **Micrograph of a typical ball bond made with 20 μm PCC wire using optimized bond parameters**

References

[1] Harman, George. 2010. *Wire Bonding in Microelectronics.* New York: McGraw-Hill Professional.

[2] Sheaffer, Michael, Lee R. Levine, and Brian Schlain. "Optimizing the wire-bonding process for copper ball bonding, using classic experimental designs." Components, Hybrids, and Manufacturing Technology, IEEE Transactions on 10, no. 3 (1987): 321-326.

[3] Wong, B. K., C. C. Yong, P. L. Eu, and B. K. Yap. "Process optimization approach in fine pitch Cu wire bonding." In Electronic Devices, Systems and Applications (ICEDSA), 2011 International Conference on, pp. 147-151. IEEE, 2011.

[4] Han, M., X. Xu, L. Hu, J. Z. Yao, and M. J. Song. "18um Pd-copper Wire Bonding Process Development." *13th International Conference on Electronic Packaging Technology and High Density Packaging (ICEPT-HDP).* Guilin, 2012. 503-506.

[5] Yeh, Jun-Hsien, and Tsung-Nan Tsai. "Optimizing the fine-pitch copper wire bonding process with multiple quality characteristics using a grey-fuzzy Taguchi method." Microelectronics Reliability 54, no. 1 (2014): 287-296.

[6] Tsai, Tsung-Nan. "A hybrid intelligent approach for optimizing the fine-pitch copper wire bonding process with multiple quality characteristics in IC assembly." Journal of Intelligent Manufacturing 25, no. 1 (2014): 177-192.

[7] Yoo, Kyung-Ah, Chul Uhm, Tae-Jin Kwon, Jong-Soo Cho, and Jeong-Tak Moon. "Reliability study of low cost alternative Ag bonding wire with various bond pad materials." In Electronics Packaging Technology Conference, 2009. EPTC'09. 11th, pp. 851-857. IEEE, 2009.

[8] Kai, Liao Jun, Liang Yi Hung, Li Wei Wu, Men Yeh Chiang, Don Son Jiang, C. M. Huang, and Yu Po Wang. "Silver alloy wire bonding." In Electronic Components and Technology Conference (ECTC), 2012 IEEE 62nd, pp. 1163-1168. IEEE, 2012.

[9] Shah, Aashish, Michael Mayer, Y. Norman Zhou, S. J. Hong, and J. T. Moon. "Low-stress thermosonic copper ball bonding." Electronics Packaging Manufacturing, IEEE Transactions on 32, no. 3 (2009): 176-184.

[10] Ng, Beng Teck, V. P. Ganesh, and Charles Lee. "Optimization of gold wire bonding on electroless nickel immersion gold for high temperature applications." In Electronics Packaging Technology Conference, 2006. EPTC'06. 8th, pp. 277-282. IEEE, 2006.

[11] Lim, Chee Chian, Yuen Chun Soh, Cher Chia Lee, and Ong Seng Lim. "Challenges of 43µm Cu bonding on very thin & softest Al bond pad structure." In Electronics Packaging Technology Conference (EPTC), 2010 12th, pp. 37-43. IEEE, 2010.

[12] Qian, Qiuxiao, Timwah Luk, and S. Irving. "Wire bonding capillary profile and bonding process parameter optimization simulation." In Thermal, Mechanical and Multi-Physics Simulation and Experiments in Microelectronics and Micro-Systems, 2008. EuroSimE 2008. International Conference on, pp. 1-7. IEEE, 2008.

[13] Nguyen, Luu T., David McDonald, Anselm R. Danker, and Peter Ng. "Optimization of copper wire bonding on Al-Cu metallization." Components, Packaging, and Manufacturing Technology, Part A, IEEE Transactions on 18, no. 2 (1995): 423-429.

[14] Yauw, Oranna, Horst Clauberg, Kuan Fang Lee, Liming Shen, and Bob Chylak. "Wire bonding optimization with fine copper wire for volume production." In Electronics Packaging Technology Conference (EPTC), 2010 12th, pp. 467-472. IEEE, 2010.

[15] Jaafar, Norhanani Binte, Wai Leong Ching, Vempati Srinivasa Rao, Chai Tai Chong, Alastair David Trigg, Guna Kanchet, and S. Sivakumar. "Fine pitch copper wire bonding process optimization with 33µm size ball

bond." In Electronics Packaging Technology Conference (EPTC), 2011 IEEE 13th, pp. 758-763. IEEE, 2011.

[16] Electronic Industries Alliance; “EIA/JEDEC Standard. Wire Bond Shear Test method. EIA/JESD22-B116A”, August 2009. USA.

[17] ASTM International; “Standard Test Methods for Destructive Shear Testing of Ball Bonds. F1269-13”, January 2013. USA.

[18] McCracken, Michael. "Assessing Au-Al Wire Bond Reliability Using Integrated Stress Sensors." (2010).

[19] Shah, A., M. Mayer, Y. Zhou, J. Persic, and J. T. Moon. “Optimization of ultrasound and bond force to reduce pad stress in thermosonic Cu ball bonding.” In Electronics Packaging Technology Conference, 2009. EPTC'09. 11th, pp. 10-15. IEEE, 2009.

[20] Nan, Chunyan, Michael Mayer, Norman Zhou, and John Persic. "Golden bump for 20micron diameter wire bond enhancement at reduced process temperature." Microelectronic Engineering 88, no. 9 (2011): 3024-3029.

[21] Medding, Jonathan, Michael Mayer. "In situ ball bond shear test for wire bond production process control." In SEMICON Singapore, 2004.

[22] Box, George EP, J. Stuart Hunter, and William G. Hunter. "Statistics for experimenters: design, innovation, and discovery." AMC 10 (2005): 12.